Organic optoelectronic device modelling: the trajectory of excitons, charges and the role of interfaces

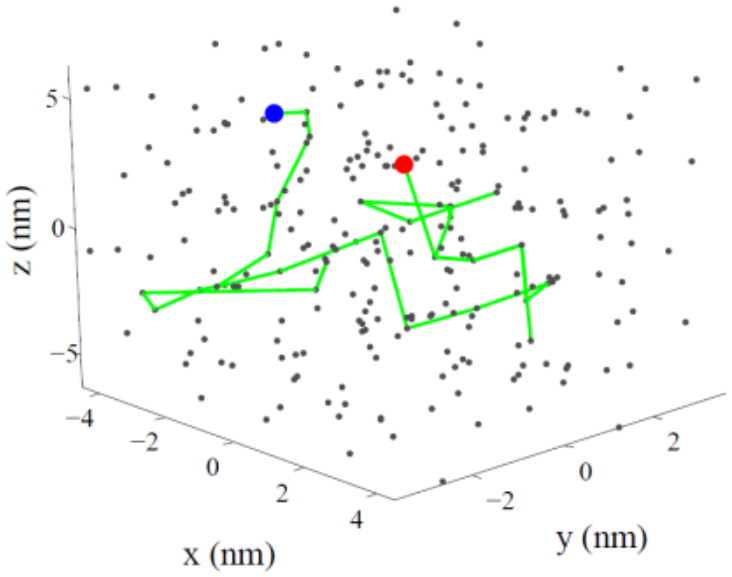

Dr. Theodoros Papadopoulos

Department of Natural Sciences

Thornton Science Park

University of Chester, U.K.

24 June, 2019

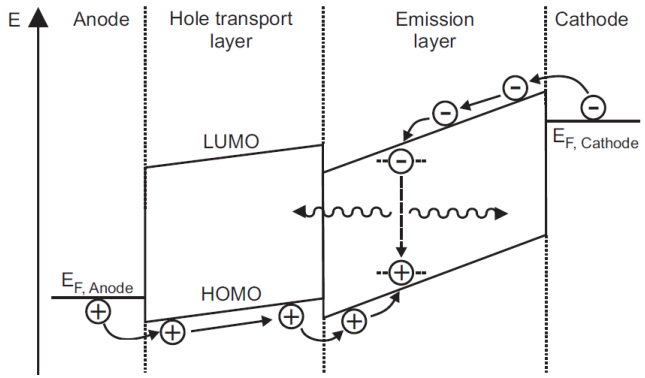

Department of Natural Sciences

University of Chester

Thornton Science Park

- Exciton transport in organic thin films [1]
- Charge transport in organic thin films [2]
- Charge transfer at organic/inorganic interfaces [3]

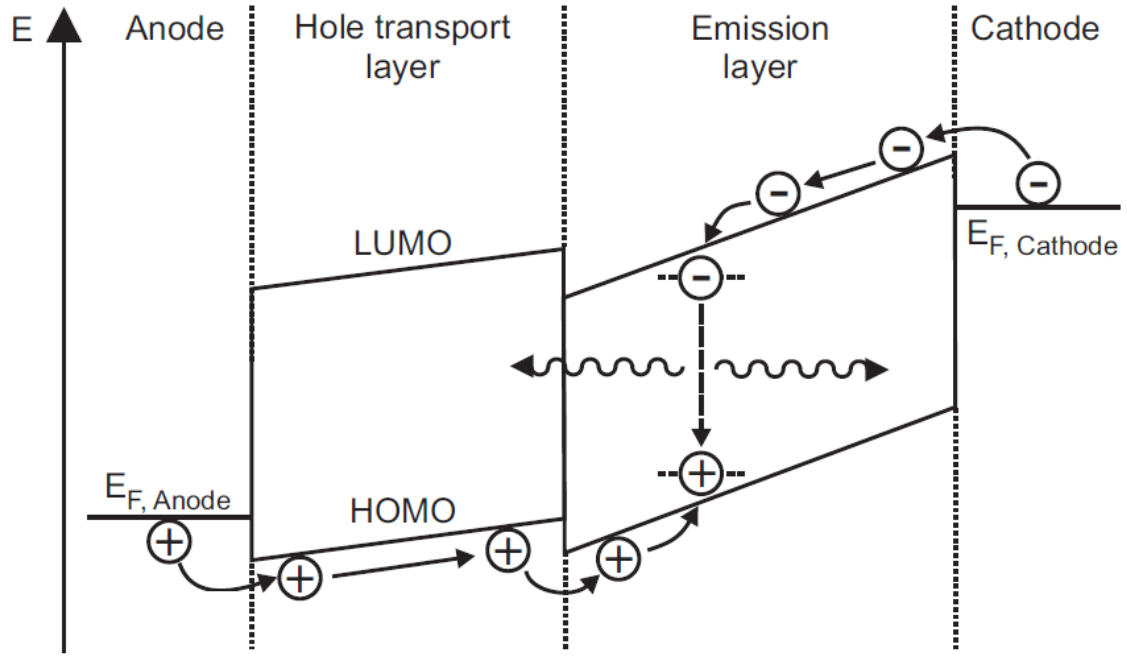

1. T. Papadopoulos, et al., *Chem. Sci*. 2, 1025 (2011).
2. S. M. Gali, et al., *J. Chem. Phys*. 147, 134904 (2017).
3. T. Papadopoulos, et al., *Adv. Funct. Mater*. 23, 6091 (2013).

OPV applications

Flexible and semi-transparent

Significant cost reduction compared to traditional solutions

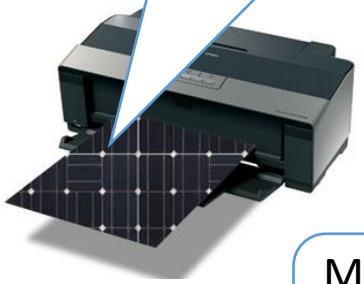

Large coating area

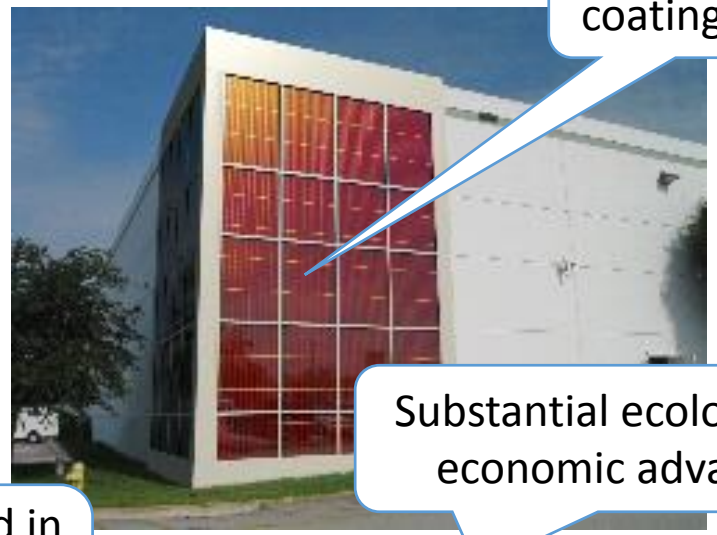

Embedded in fabrics

Manufactured in a continuous printing process

Substantial ecological and economic advantages

OLED applications I

Lightweight and can cover almost any surface

Embedded in fabrics

Flexible giving rise to artistic design with light

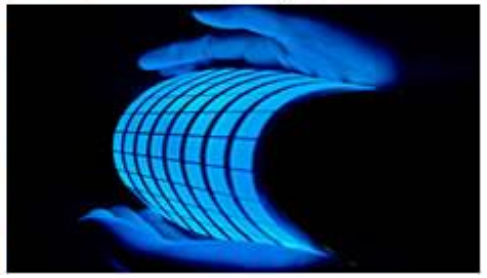

Wider viewing angles and improved contrast (no backlight, correct colors, true black)

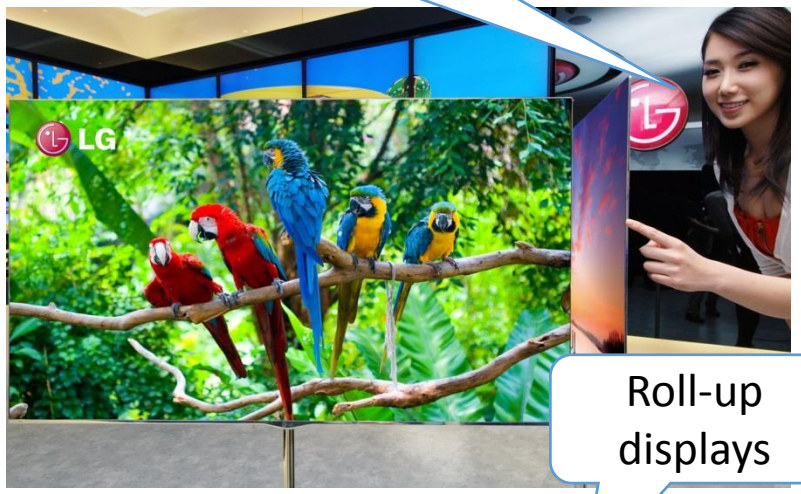

Roll-up displays

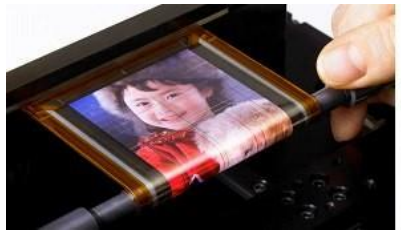

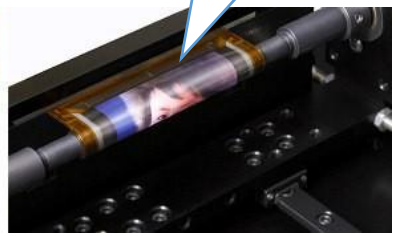

Not possible with current inorganic LED technology

Part I: Charge transfer at metal-oxide/organic interfaces

- We would like to understand the role of transition metal oxides in the performance of organic optoelectronic devices.
- Adsorb of a π-conjugated organic hole transport layer.
- Effect of stoichiometric and under-stoichiometric metal-oxide surfaces on energy level alignment with the hole-transport layer.
- Evaluate the experimentally observed gap-state density after adsorption of the organic film on the metal oxide.

What is the influence of oxygen vacancies on the substrate surface?

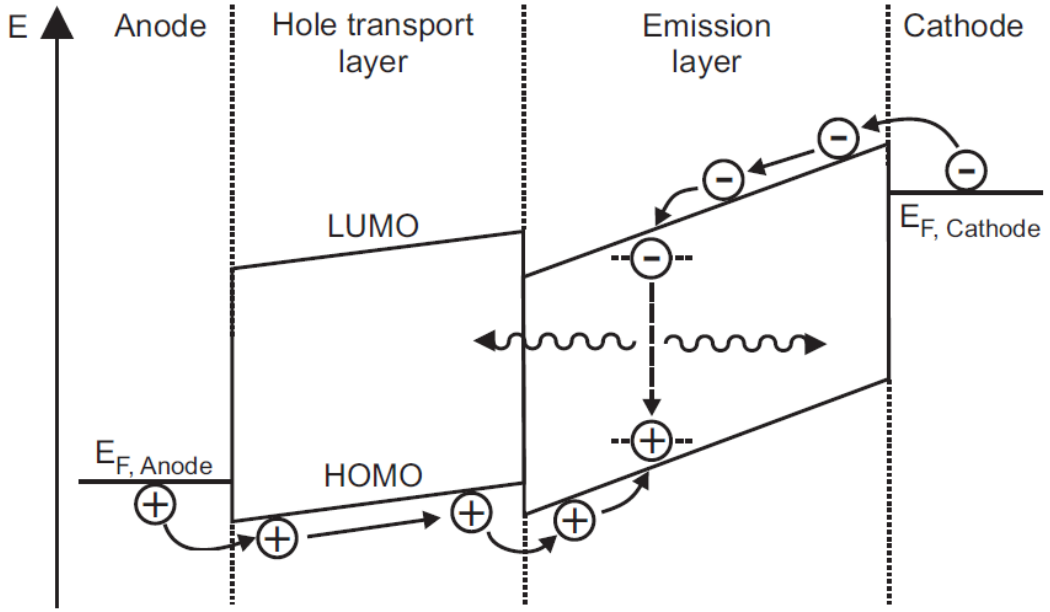

- Y. Zhou et al., *Science* 336, 327 (2012).
- T. Papadopoulos et al., *Adv. Funct. Mater*. 23, 6091 (2013).
- M.-K. Lin, et al., *Phys. Rev. B* 95, 085425 (2017).

Department of Natural Sciences

University of Chester

Thornton Science Park

The system studied

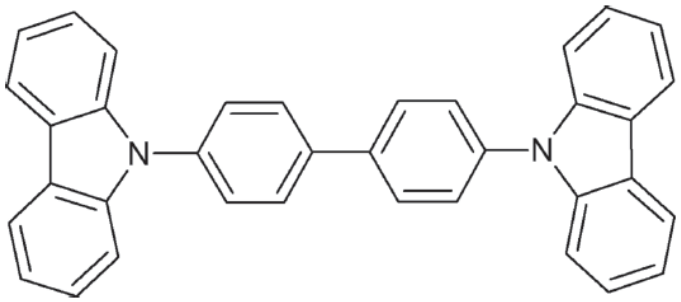

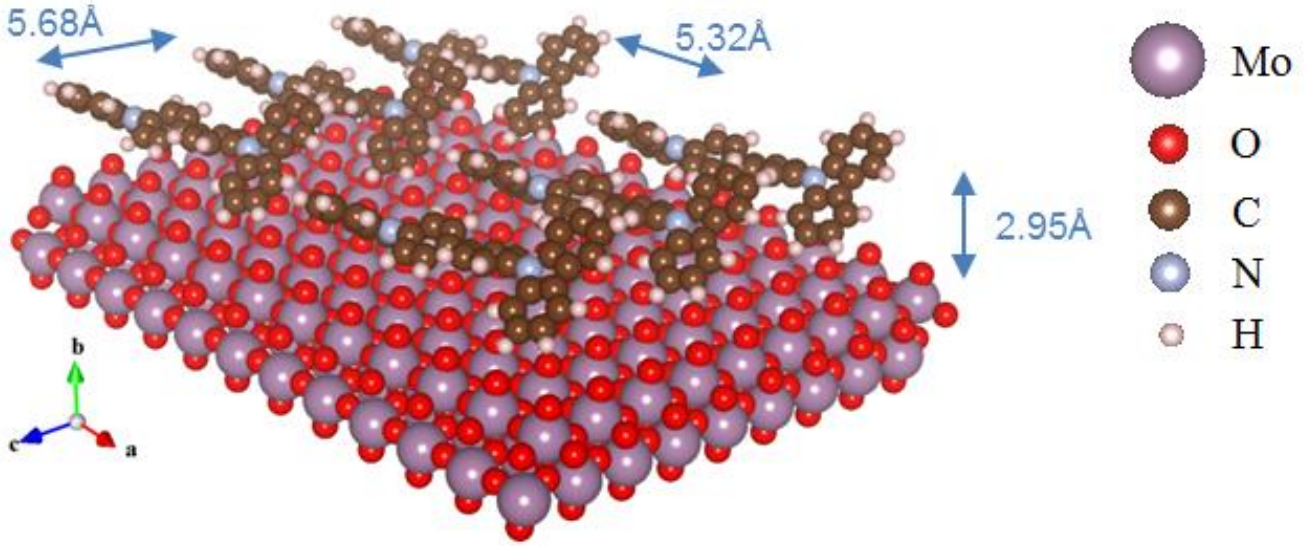

- Interfacial system: MoO_3/4,4′-N,N′-dicarbazole-biphenyl (CBP)
- We consider both stoichiometric MoO_3 (010) and under-stoichiometric MoO_x (010) surfaces as well as their interfaces with CBP.

Energy level alignment via UPS

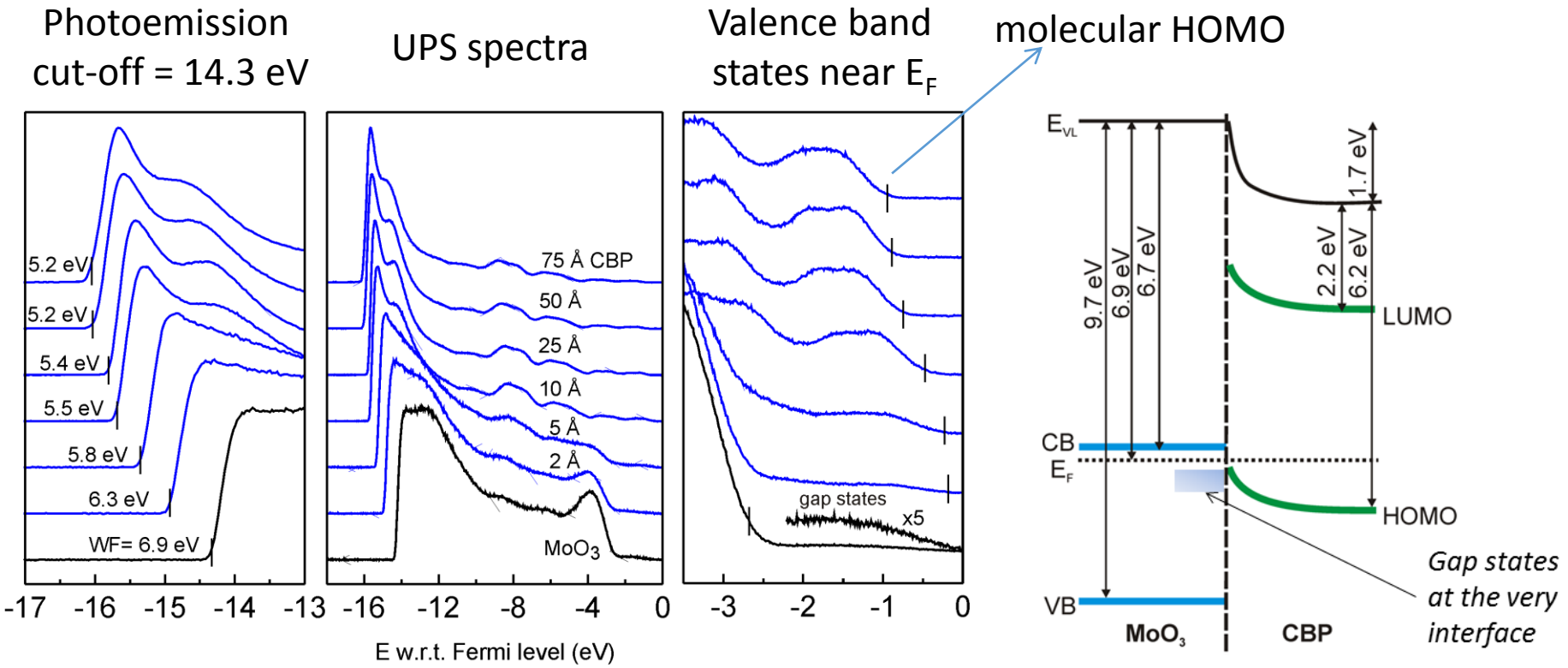

- Band bending occurs as a result of a p-doping effect at the interface causing the HOMO level to move downwards away from E_F.
- Gap states are centered near -1.4 eV and extend up to E_F.

UPS spectra and experimental energy level diagram provided by the group of Prof. Antoine Kahn, Princeton University

Energy level alignment via UPS

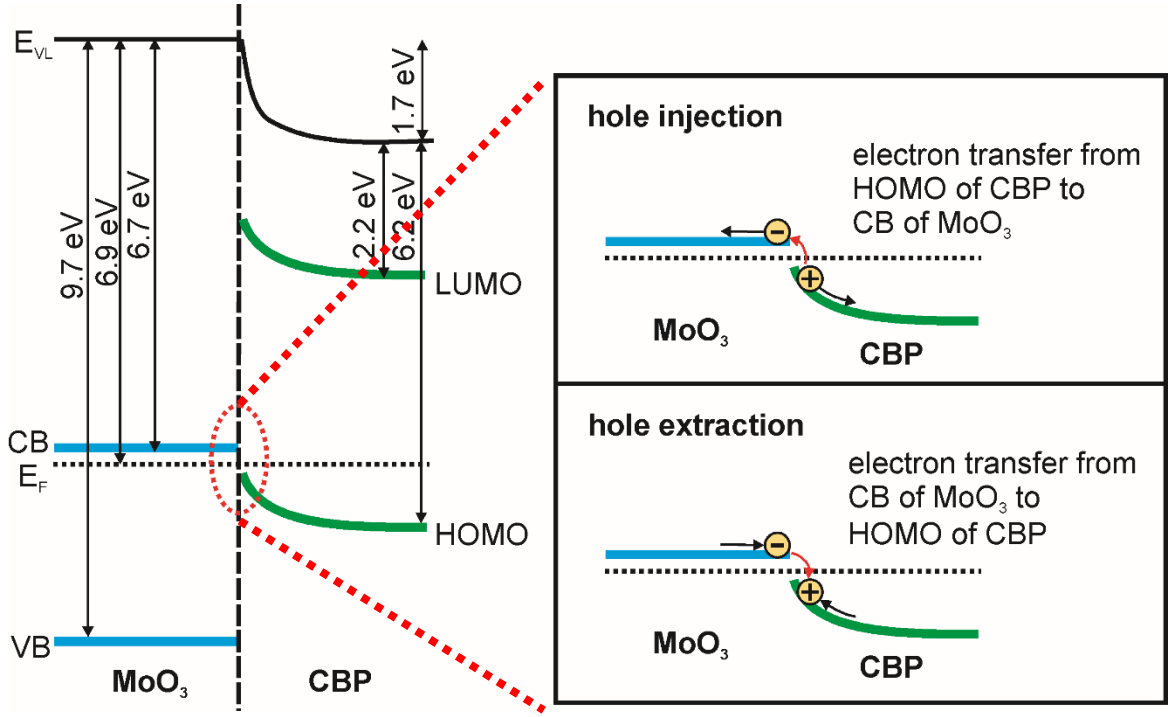

OLED

OPV

- What is the origin of the gap states observed via UPS?
- What would be their effect of energy level alignment?
- Could we quantify this effect? Can theory help?

Experimental energy level diagram provided by the group of Prof. Antoine Kahn, Princeton University

Department of Natural Sciences
University of Chester
Thornton Science Park

DOS of the MoO_3(010) surface

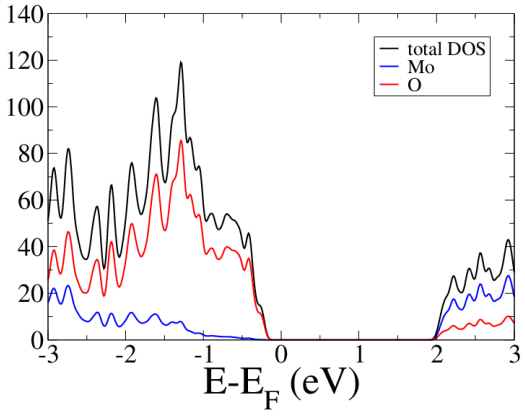

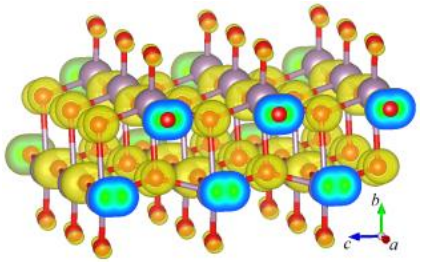

Charge density corresponding to the states in a range of 0.15eV below E_F.

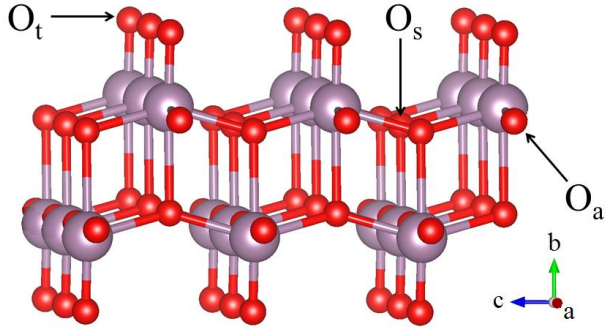

MoO_3 (010) surface	EA (eV)	IP (eV)
Theory (DFT-PBE)	6.3	8.6
Experiment*	6.7	9.7

- There seem to be no gap-states observed for the stoichiometric MoO_3.
- VBM: Major contributions on the charge density come from Oxygen 2*p* electrons with nearly no contribution from Mo 4*d* electrons.
- CBM: Major contribution from Mo 4*d* states and a smaller contribution from O 2*p* states.
- What should we expect if we introduce oxygen vacancies?

* J. Meyer et al., APL **96**, 133308 (2010)

DOS for the MoO_x surface: O_t vacancy

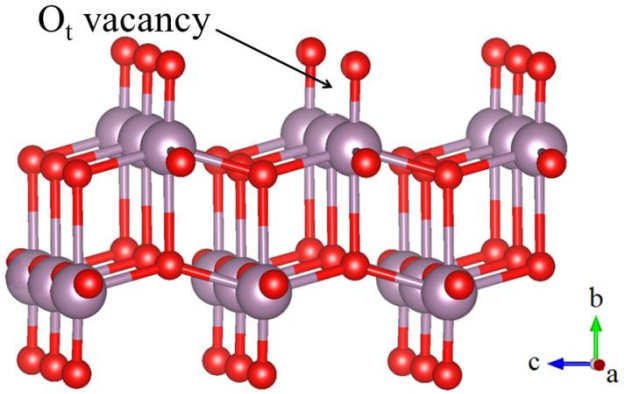

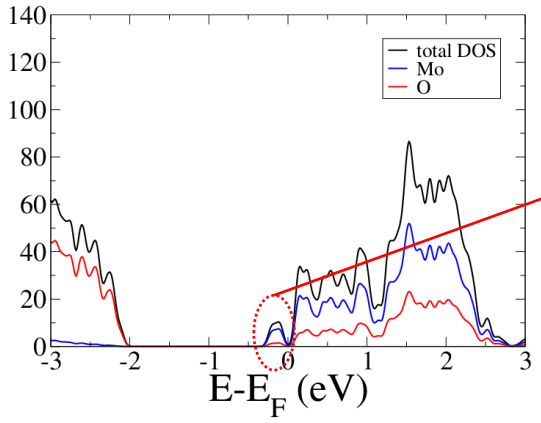

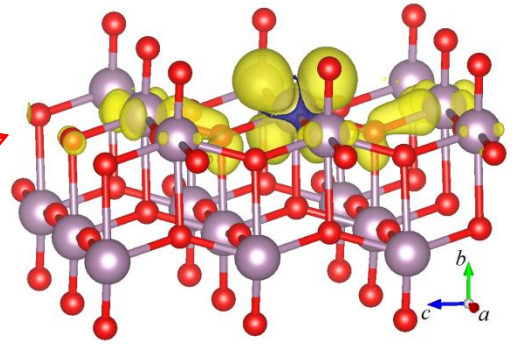

Charge density corresponding to the O-vacancy states right below E_F, showing the Mo unsaturated bonds.

MoO_x surface	EA (eV)	IP (eV)	Φ (eV)
Theory (DFT-PBE)	6.02	8.18	6.15

- MoO_x(010) surface, x = 2.94, close to experimental estimation by Cho et al., JPCC 114, 18252 (2010).
- DOS shows n-type behavior with shallow states appearing ~0.1 eV below CB edge with major contribution form Mo 4*d* states.
- Experimental work function: Φ = 6.86 eV by Meyer et al., APL 96, 133308 (2010).

DOS for the MoO_x surface: O_a and O_s vacancy

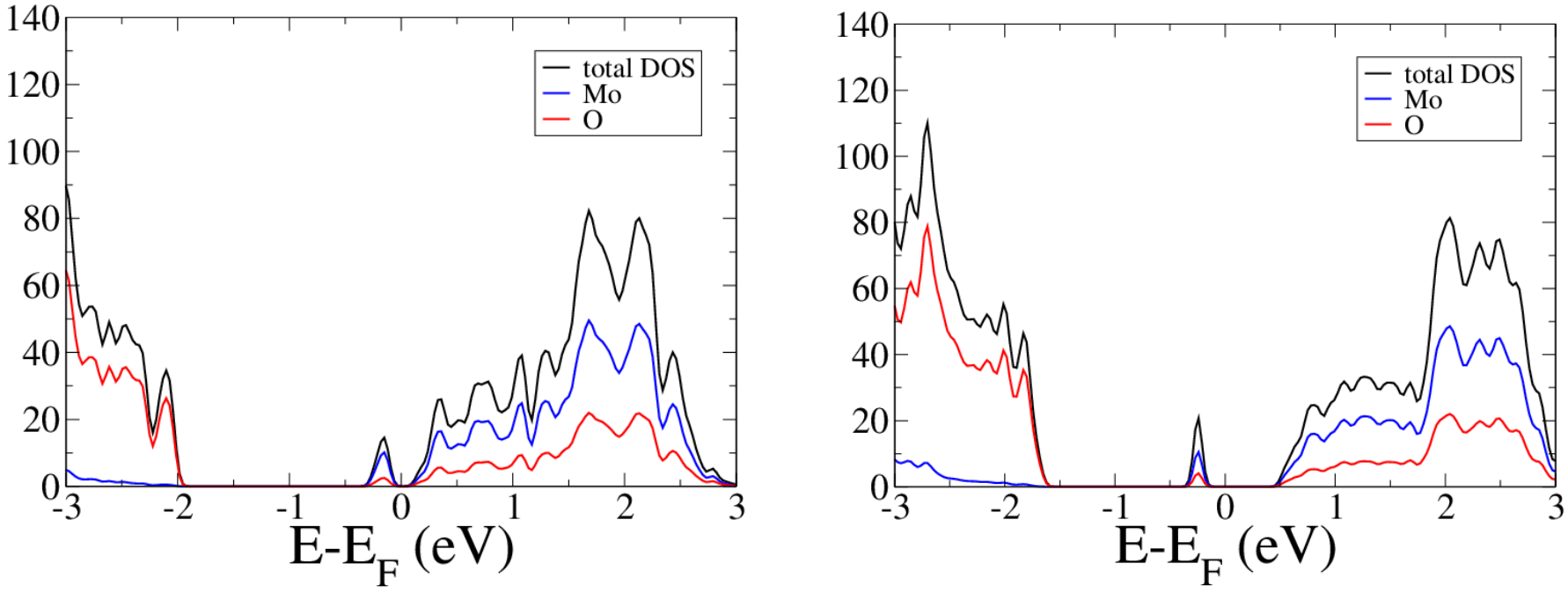

- O_t and O_a vacancies contribute to the experimentally observed gap states near E_F (O_a are ~0.3 eV below the CB edge).
- O_s vacancies contribute to almost mid-gap states, ~0.75 eV below CB edge.
- In practice a combination of different types of O vacancies could induce a complex geometry that contributes to the gap states centered at ~ 1.4 eV below E_F, as observed via UPS measurements.

Energy level alignment

Energy level alignment via UPS

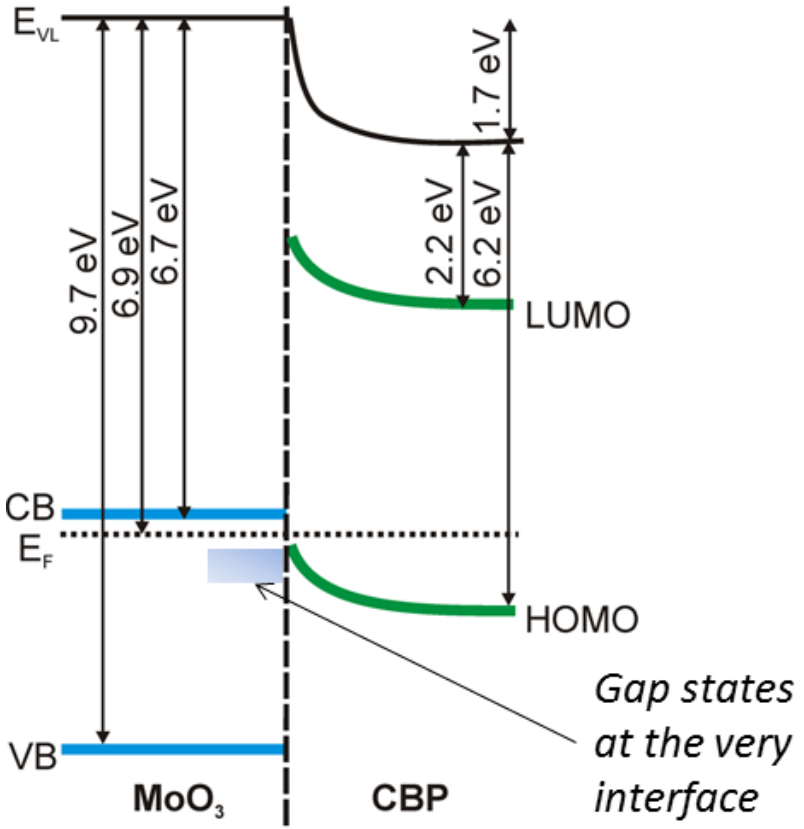

Theoretical DOS of the MoO_x surface

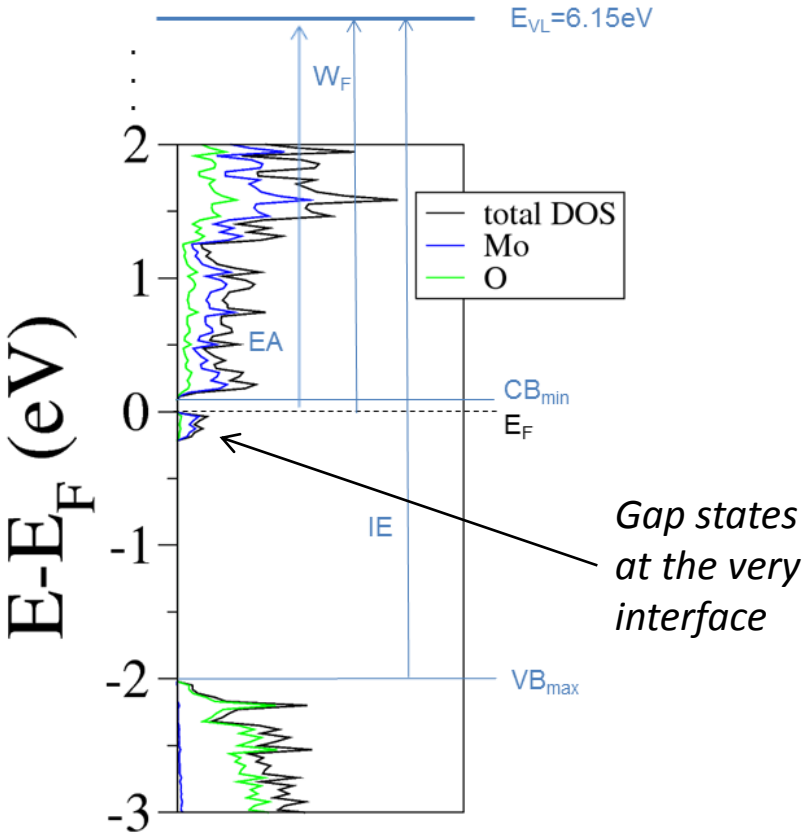

- Experimentally we can see that there is a favorable energy level alignment at the interface.
- Could we quantify and understand this effect theoretically after the adsorption of CBP?

DOS for the CBP/MoO_3 interface

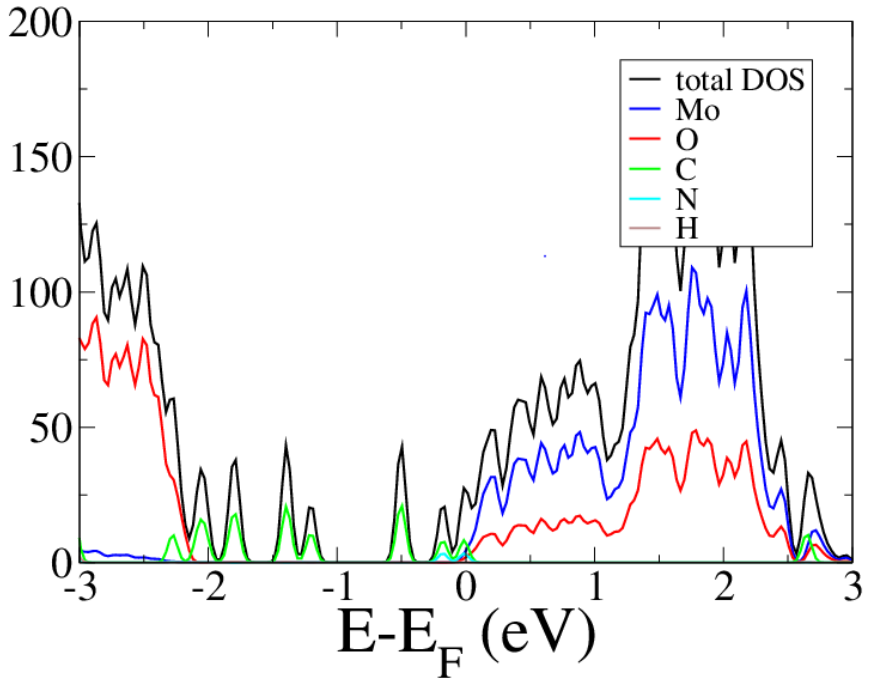

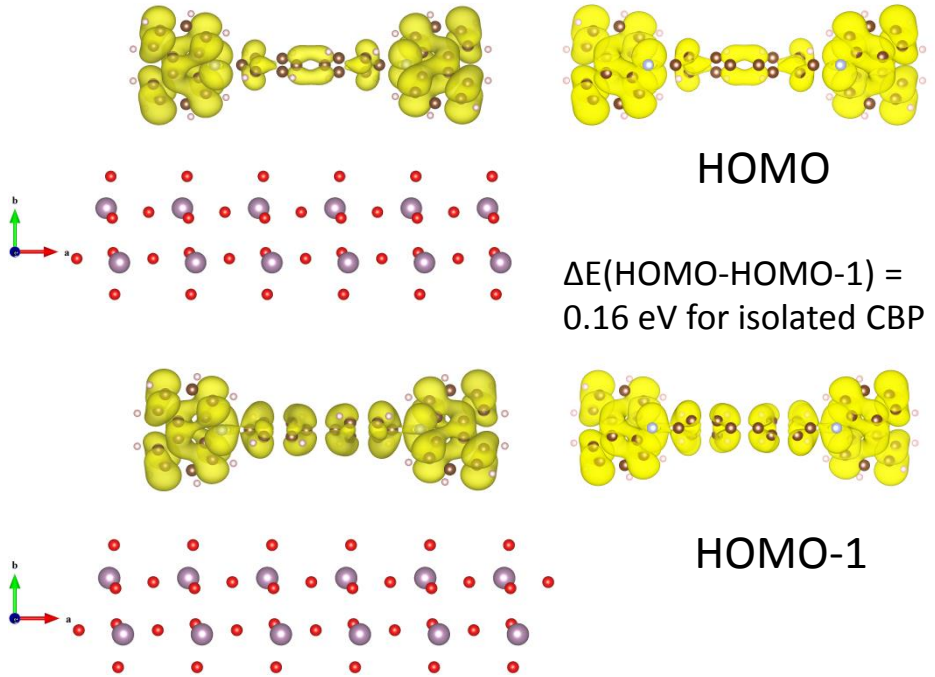

- Fermi level is right below the CB edge.
- Two molecular states, separated by 0.16 eV, (in green) have the same character and correspond to the HOMO and HOMO-1 of an isolated CBP (consistent with UPS showing HOMO close to CB edge).
  - The energy difference of HOMO and HOMO-1 for isolated CBP is 0.14 eV, close to the value for CBP adsorbed on MoO_3.

DOS for the CBP/MoO_x interface

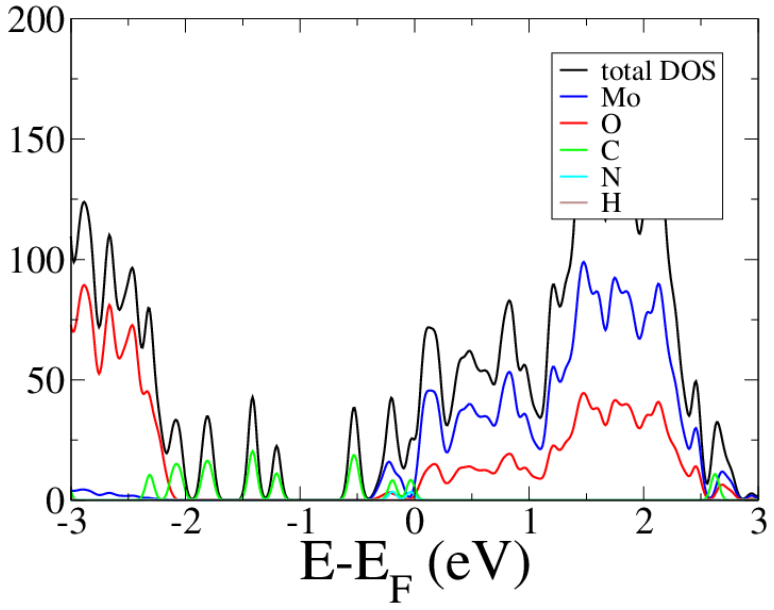

- Similar DOS apart from the states below E_F.
- These are highly mixed levels associated with contributions of both the molybdenum atoms from the MoO_x slab and the carbon and nitrogen atoms belonging to the CBP monolayer.
- The HOMO of CBP is found to almost align with E_F, leading to a *nearly* zero barrier for charge collection/injection from/to the MoO_x surface.

Charge transfer at the interface

$$\Delta\Phi = \Delta V_{int.dip} + \Delta V_{mol.} + \Delta V_{surf.rel.}$$

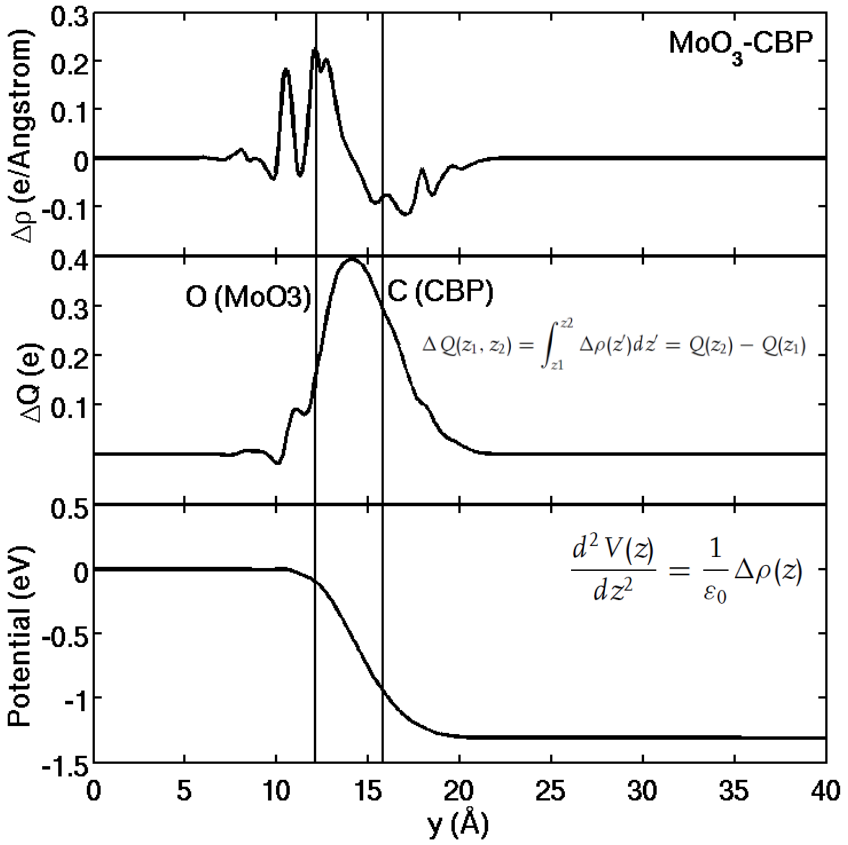

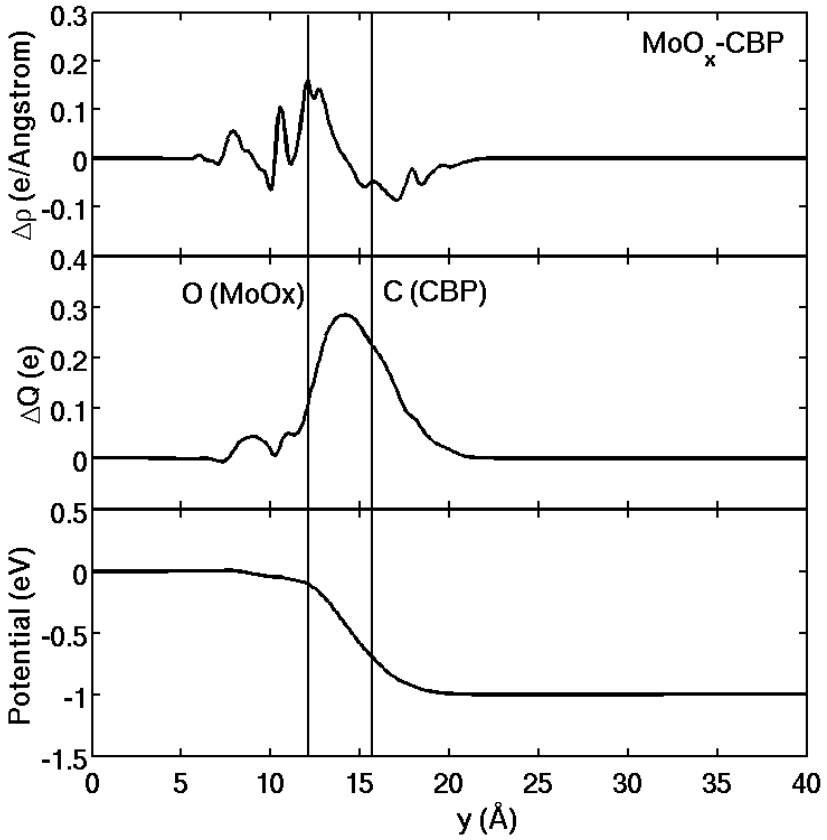

- The sum of the above three components is $\Delta\Phi$ = -1.22 eV and $\Delta\Phi$ = -1.06 eV for the MoO3/CPB and MoOx/CPB interfaces respectively.
- In good agreement with experiment for CBP deposition of 5Å, i.e. $\Delta\Phi$ = -1.10 eV

Conclusions of Part I

- Terminal and asymmetric oxygen vacancies seem to be related to gap states just below the MoO_x CB edge.
- Symmetric oxygen vacancies show their “fingerprint” about 0.75 eV below the CB edge, almost at mid-gap.
- There is a combined contribution to the broad UPS gap states from all the above types of O vacancies.
- The HOMO of CBP is found to almost align with E_F, leading to a *nearly* zero barrier for charge collection/injection from/to the MoO_x surface.
- Molybdenum trioxide can be a suitable anode candidate to realize efficient charge injection/collection processes in metal-oxide/organic interfaces.

Part II: Exciton migration in organic thin films

- Present a method to extract singlet exciton diffusion dynamics combining MD simulations, quantum chemical calculations and KMC modelling.
- Our aim is to investigate how sensitive are exciton transport properties to changes in oligomeric morphology and temperature.
- We demonstrate that positional and orientational disorder does not seem to affect the ability of excitons to diffuse.
- On the other hand, when energetic disorder becomes dominant, a significant decrease on the exciton diffusion length is observed. Would this be relevant?

What is the influence of positional and energetic disorder?

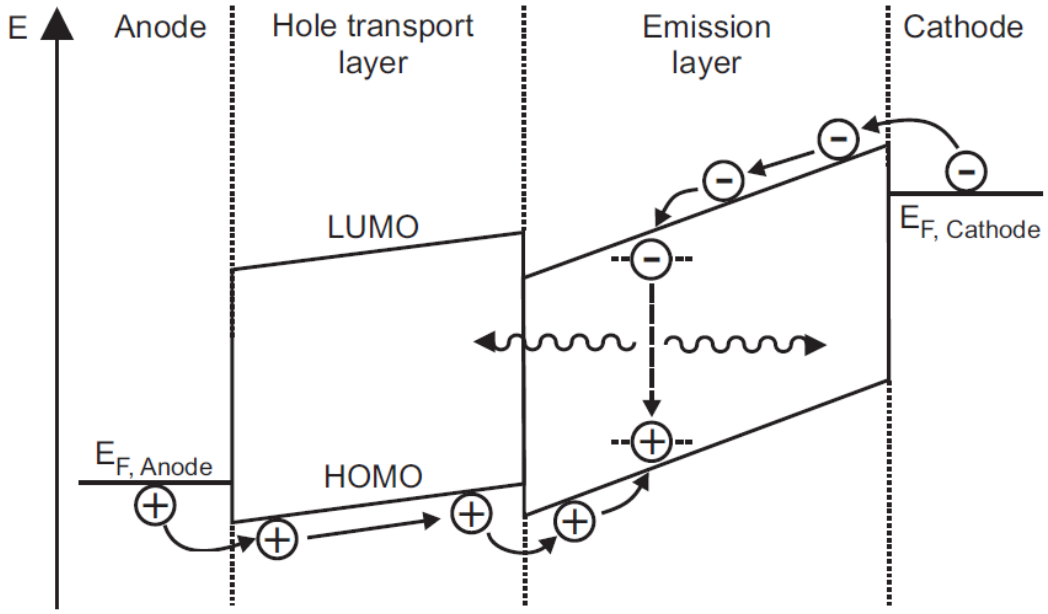

T. Papadopoulos, et al., *Chem. Sci*. 2, 1025 (2011).

Department of Natural Sciences
University of Chester
Thornton Science Park

Motivation for the system studied

We use indenofluorene trimers (IF3)

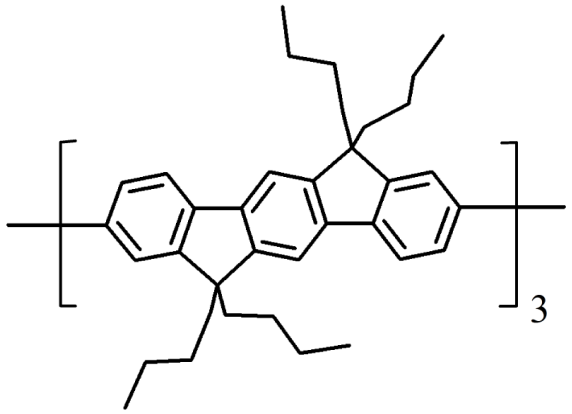

- Indinofluorene oligomers are blue and violet emitters
- Their morphology is well characterised experimentally, via wide angle X-ray scattering
- Promising for optoelectronic device applications

Theoretical approach

- We use Molecular Dynamics to extract the thin film morphology (NAMD, CHARMM)
- Exciton transfer rates are then extracted using an improved Förster approach:
  - The excitonic coupling between chromophores is:

$$V_{ij} = \frac{1}{4\pi\varepsilon_0} \sum_m \sum_n \frac{\rho_i(m)\rho_j(n)}{r_{mn}}$$

  - The hopping rate between donor and acceptor is: $k_{ij} = \frac{2\pi}{\hbar} \left|V_{ij}\right|^2 J_{ij}$

  where $\rho_i(m)$ is the atomic transition density on each chromophore (INDO/CCSD level), J_{ij} the spectral overlap, m, n the atom sites and i, j the donor and acceptor chromophore sites.

  - The donor i is on its 1st excited state and the acceptor j on its ground state.

Theoretical approach

- We use Kinetic Monte Carlo (KMC) modelling to follow the time evolution of the energy transfer:
  - A waiting time is calculated for each possible event: $\tau_{ij} = \frac{1}{k_{ij}} \ln(X)$, where X is a random number uniformly distributed between 0 and 1.
  - A recombination time is calculated as: $\tau_R = \tau_L \ln(X)$, where the lifetime of a singlet exciton localised on an IF3 was measured as $\tau_L = 655$ ps.
- Exciton diffusion dynamics are extracted as follows:
  - The diffusion length for each trial is: $L_d^{trial} = \sqrt{\Delta x^2 + \Delta y^2 + \Delta z^2}$
  - Finally we will have: $L_d = \langle L_d^{trial} \rangle$

  where $\Delta x, \Delta y, \Delta z$ is the spatial difference between the initial and final point on the exciton trajectory.

T dependent thin film morphology

300K

400K

500K

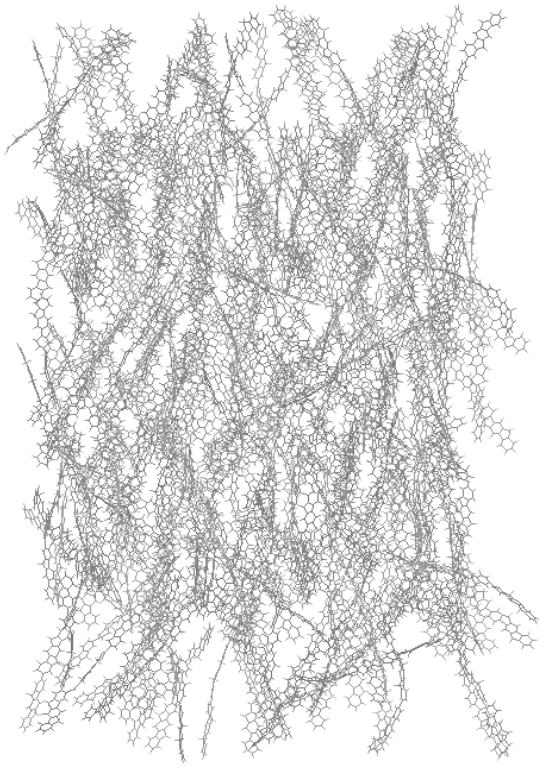

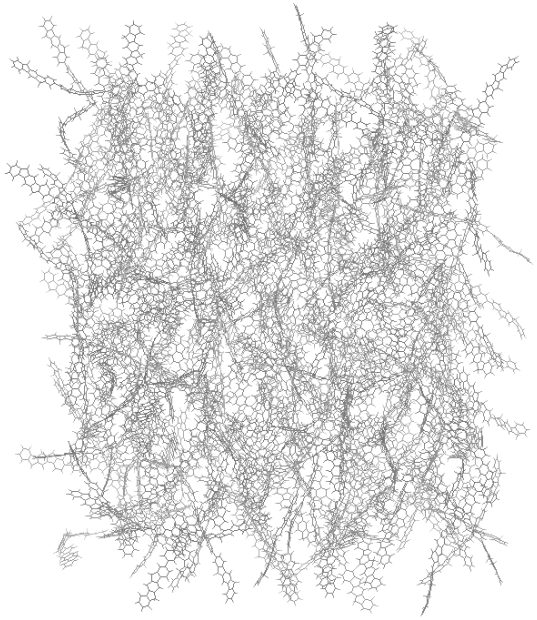

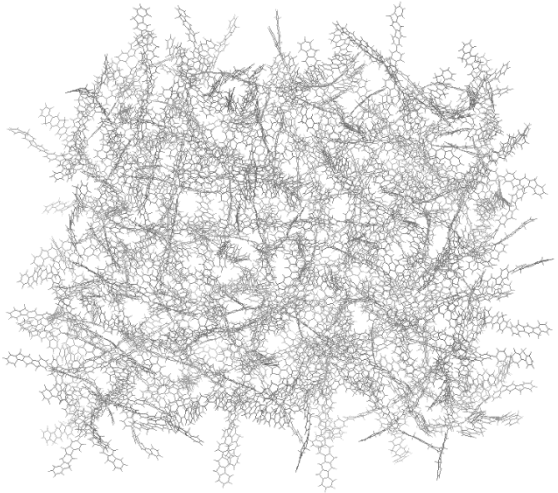

z

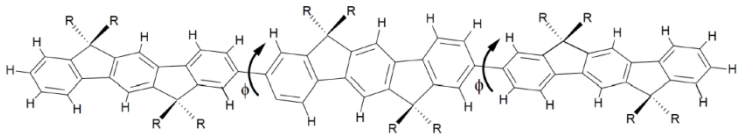

Excitonic coupling

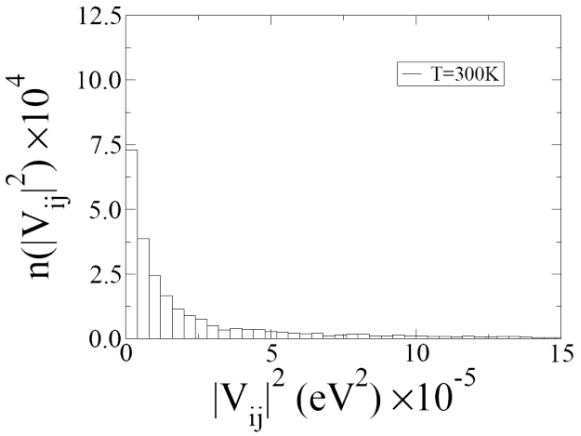

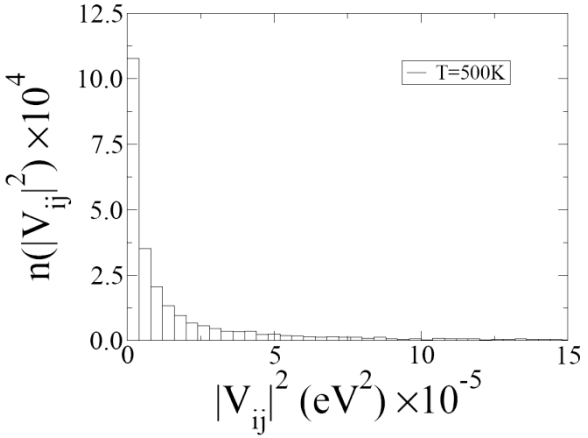

Distributed monopole approximation

$$V_{ij} = \frac{1}{4\pi\varepsilon_0}\sum_m\sum_n \frac{\rho_i(m)\rho_j(n)}{r_{mn}}$$

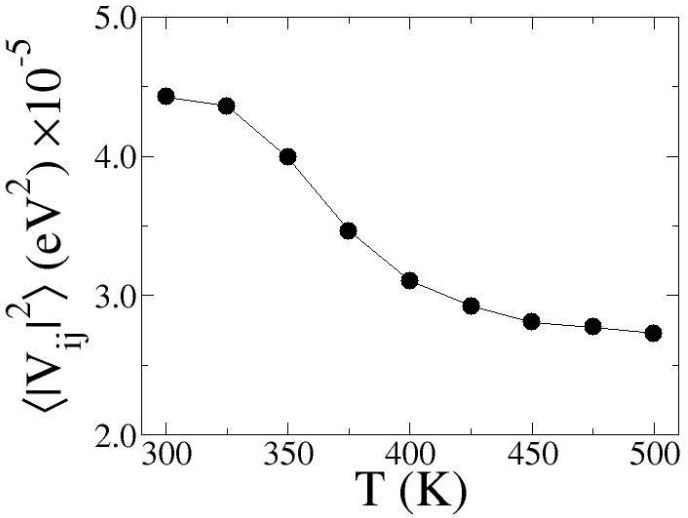

The excitonic coupling is decreasing as a function of T

$\rho_i(m)$ is the atomic transition density on each chromophore (INDO/CCSD level), J_{ij} the spectral overlap, m, n the atom sites and i, j the donor and acceptor chromophore sites. The donor i is on its 1st excited state and the acceptor j on its ground state.

Department of Natural Sciences
University of Chester
Thornton Science Park

$|V_{ij}|^2$ as a function of θ

The hopping rate between donor and acceptor

$$k_{ij} = \frac{2\pi}{\hbar}|V_{ij}|^2 J_{ij}$$

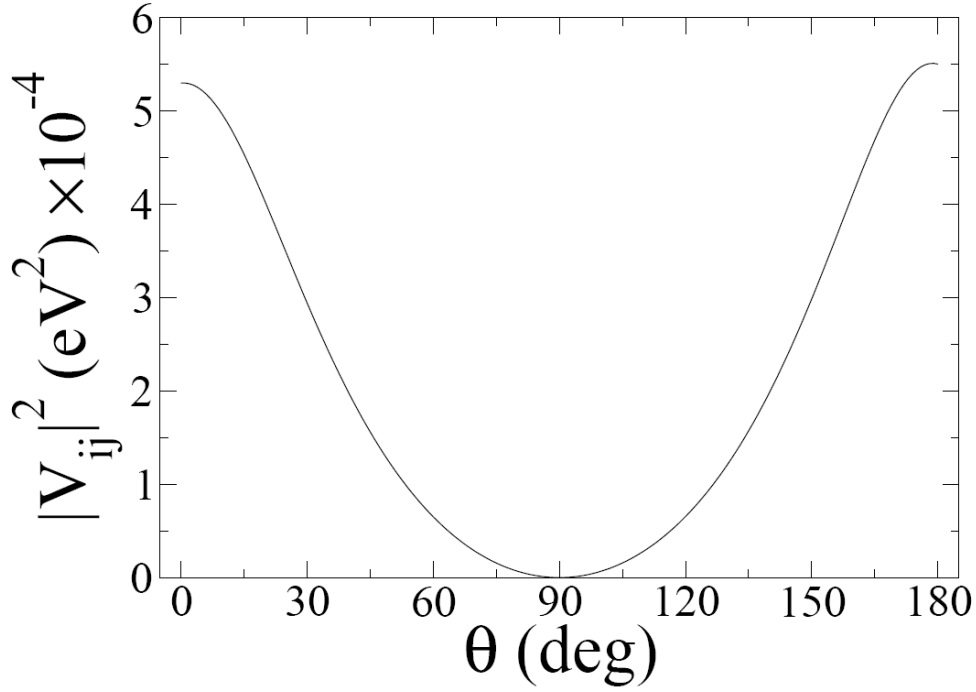

θ is the rigid body rotation angle around the axis connecting the centre of masses of two IF trimers

Spectral overlap J_{ij}

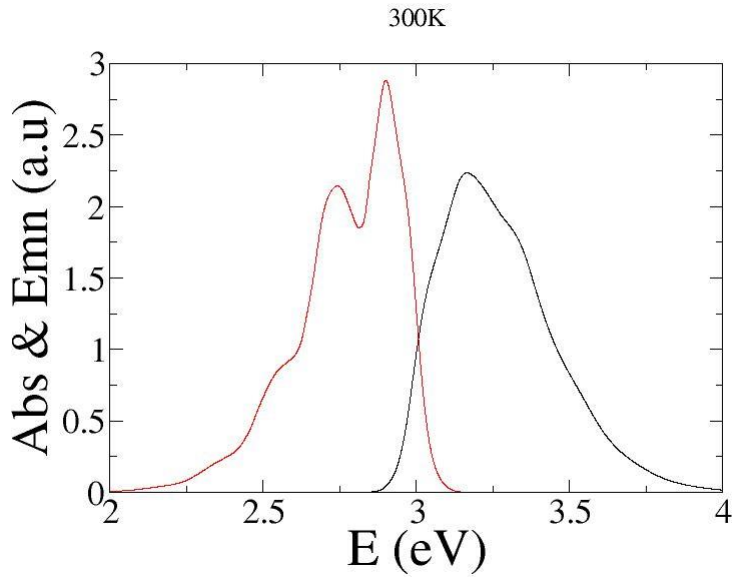

Spectral overlap J_{ij}

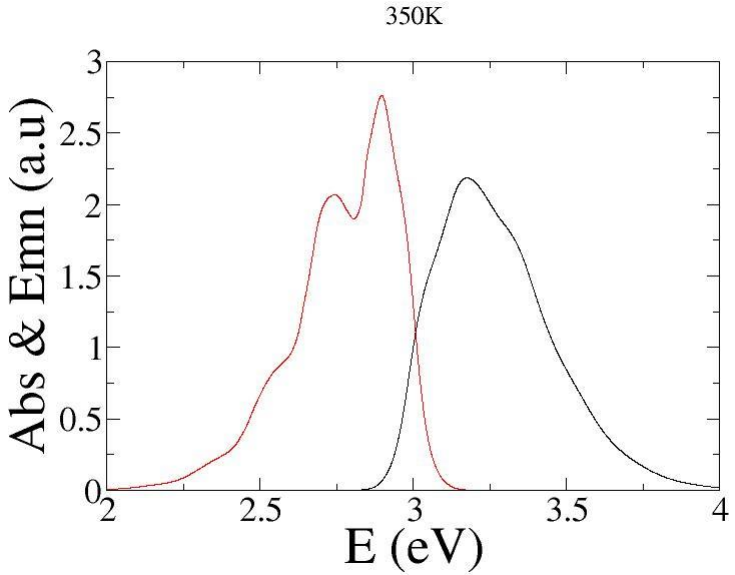

Spectral overlap J_{ij}

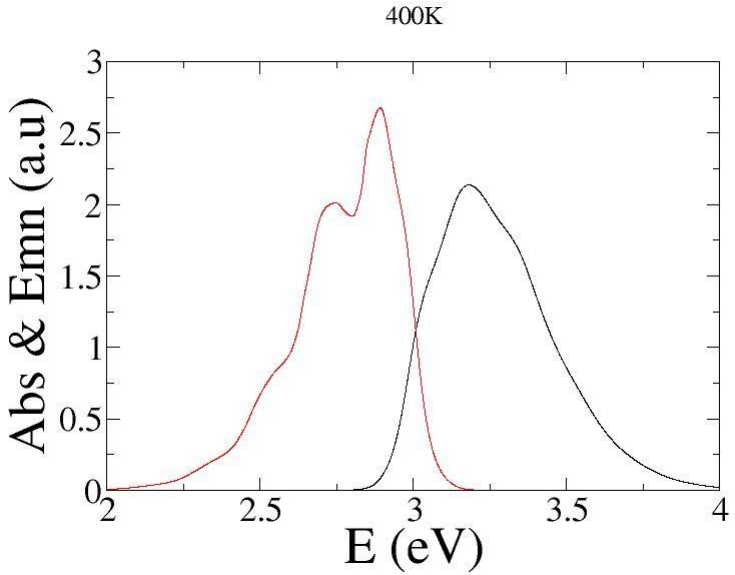

Spectral overlap J_{ij}

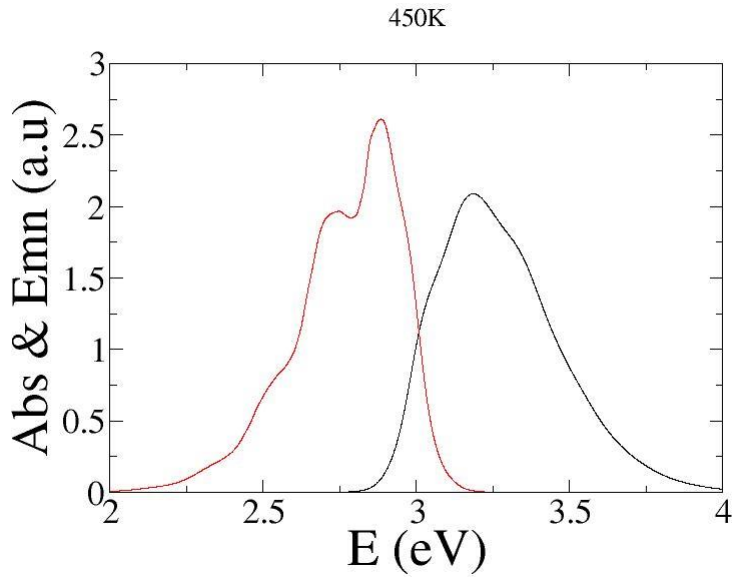

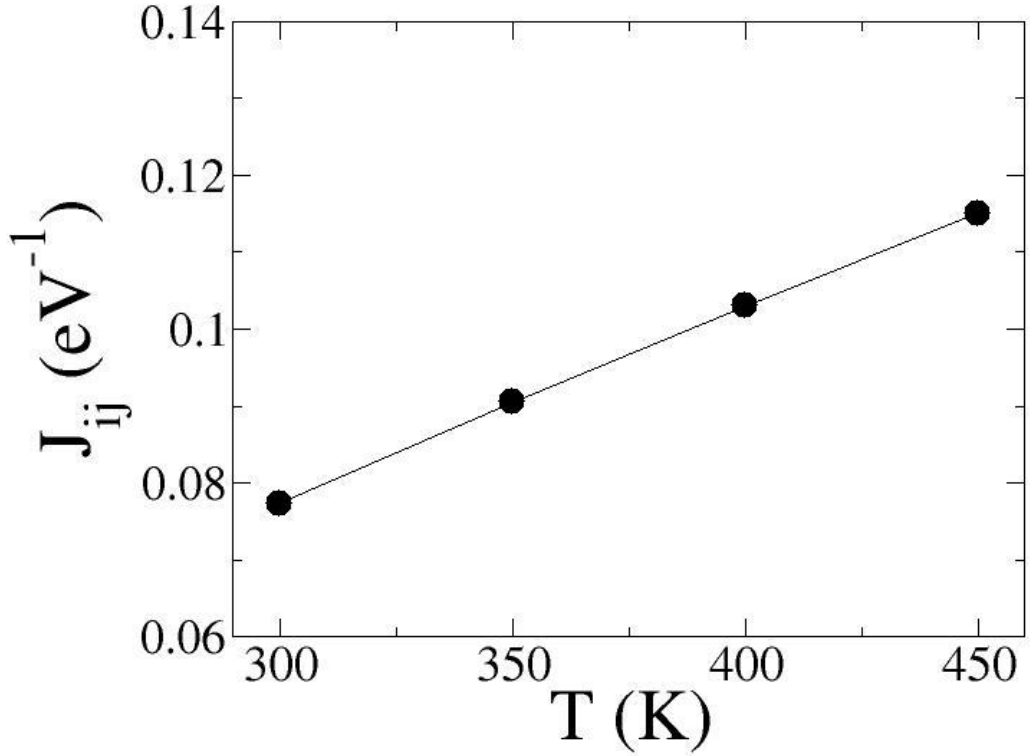

The spectral overlap is found to be increasing as a function of T.

Hopping rate k_{ij}

What would be the effect on k_{ij}?

$$k_{ij} = \frac{2\pi}{\hbar}\left|V_{ij}\right|^2 J_{ij}$$

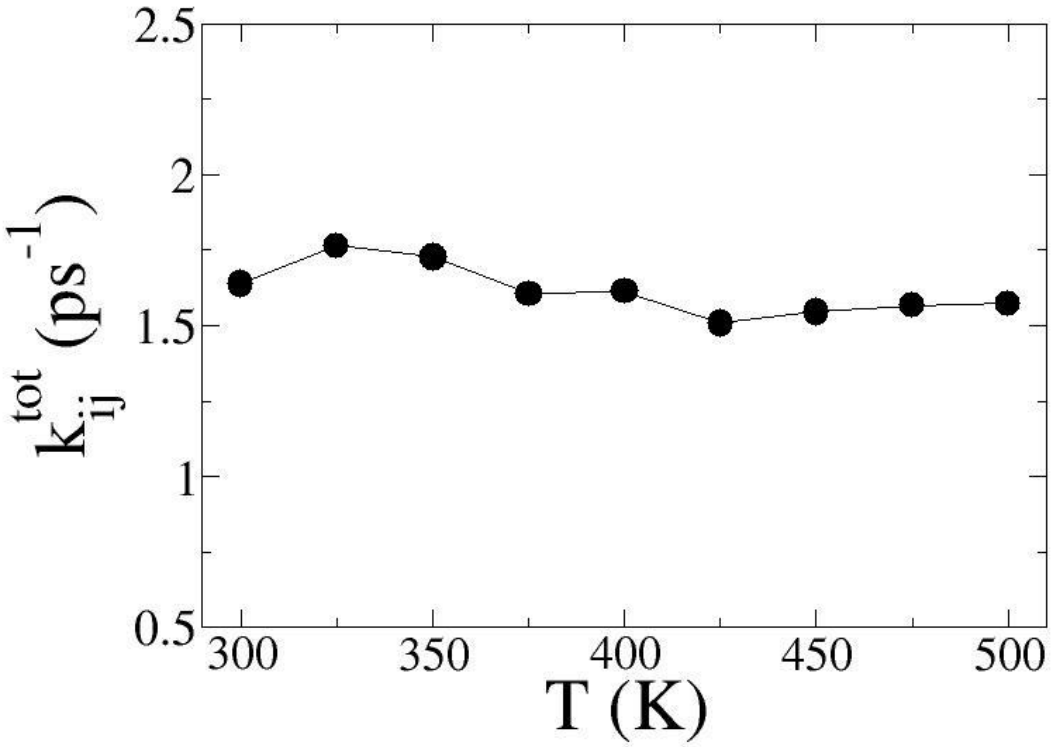

Diffusion length L_d

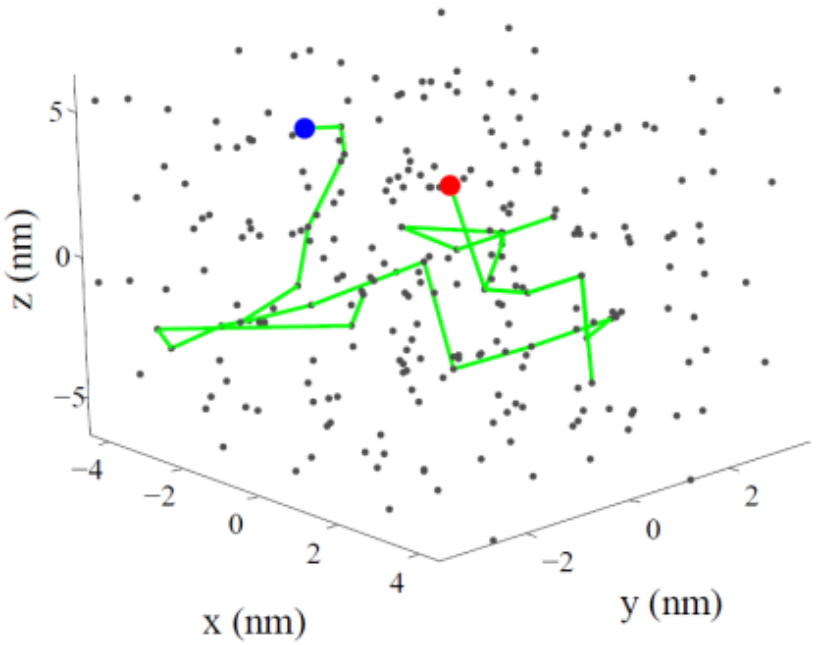

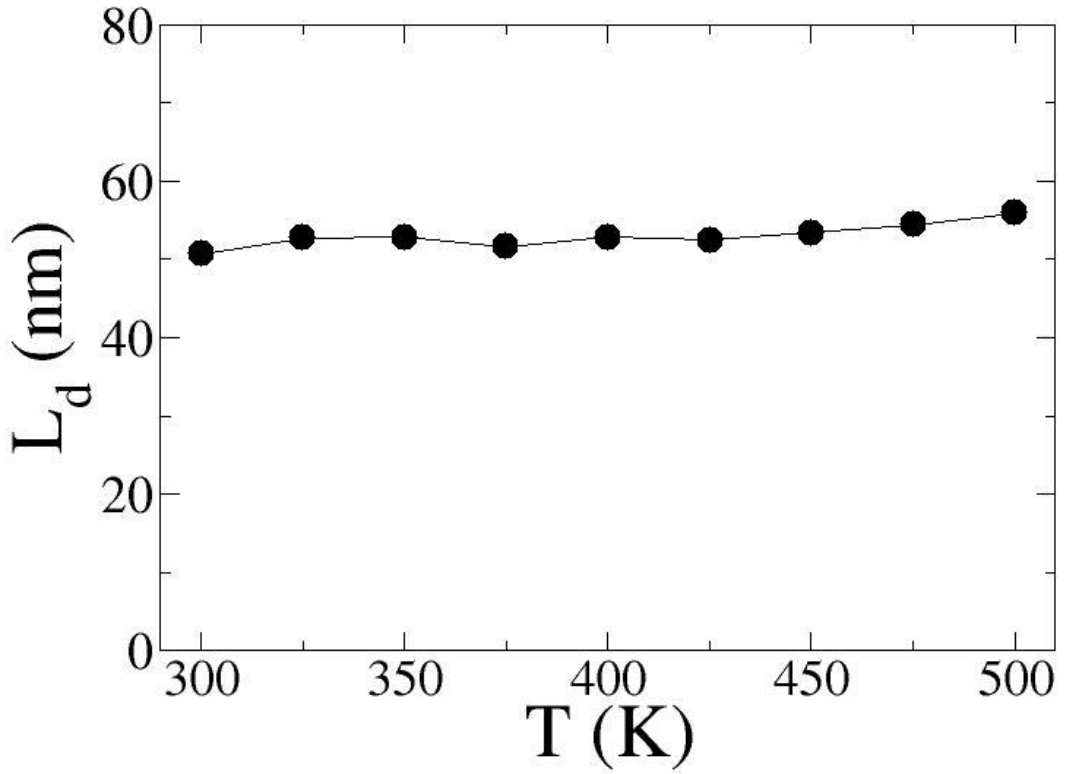

L_d stays constant as T increases due to the cancelling effect of the decrease in $|V_{ij}|^2$ and the increase in J_{ij} as a function of temperature.

$$L_d^{trial} = \sqrt{\Delta x^2 + \Delta y^2 + \Delta z^2}$$

$$L_d = \langle L_d^{trial} \rangle$$

where $\Delta x, \Delta y, \Delta z$ is the spatial difference between the initial and final point on the exciton trajectory.

Department of Natural Sciences
University of Chester
Thornton Science Park

Diffusion length along x-, y-, and z-axis

- When the smectic phase on the morphology is still valid, we observe that the diffusion length is greater along the z-axis.
- As T is increased the morphology becomes isotropic.

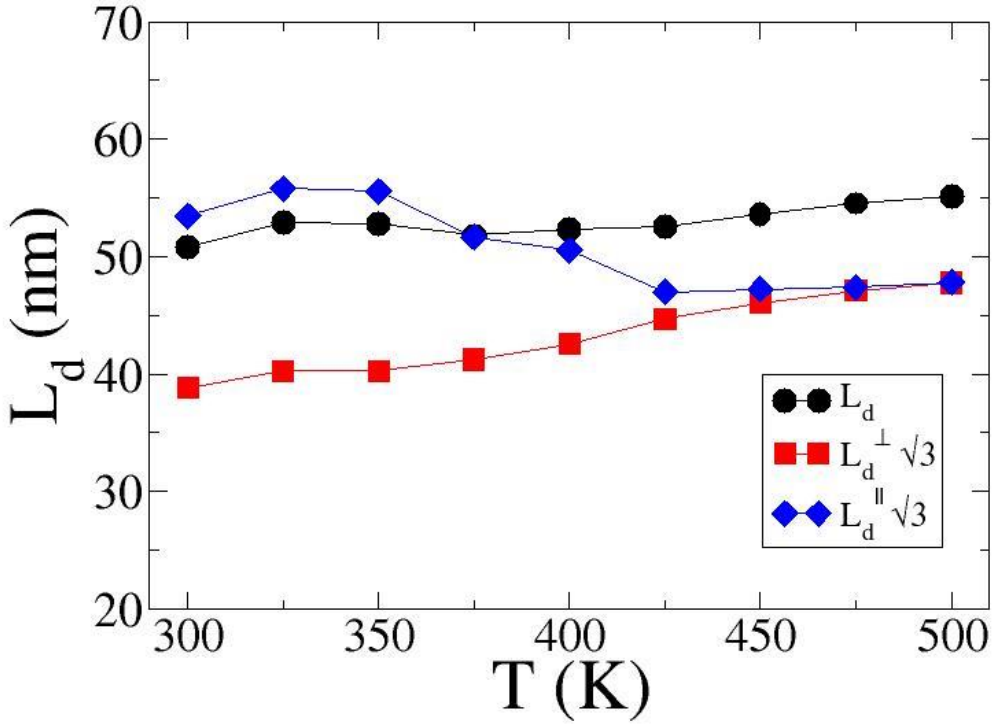

Energetic disorder

Inhomogeneous energetic disorder is introduced through a random rigid shift on the chromophore spectra. Hence a randomly chosen spectral overlap is taken for each hopping rate between donor and acceptor which depends on the width σ of a Gaussian distribution.

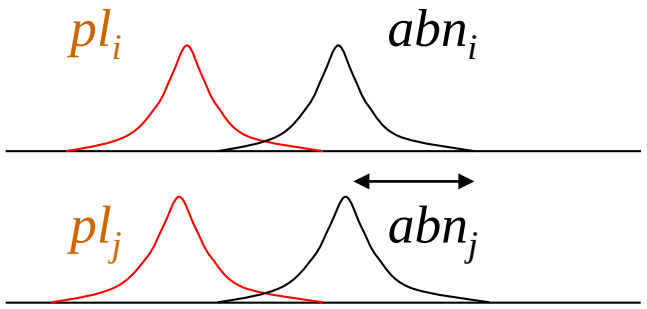

i $k_{ij} = f[|V_{ij}|^2, J(pl_i, abn_j)]$

j $k_{ji} = f[|V_{ji}|^2, J(pl_j, abn_i)]$

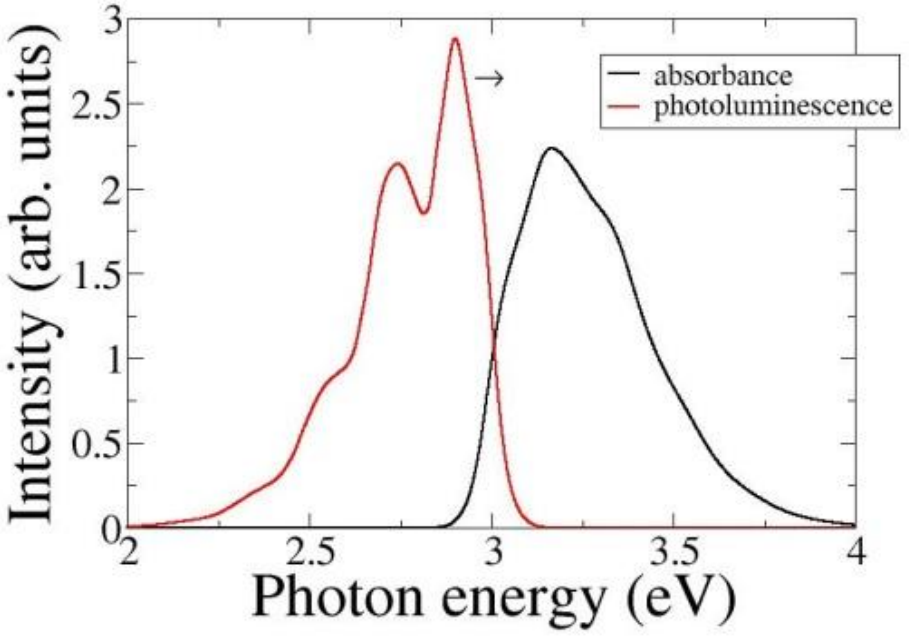

Influence on diffusion length

Each random shift is chosen for each chromophore from a Gaussian distribution of width σ centred on $\mu = 0.0$ eV.

Relevant disorder range

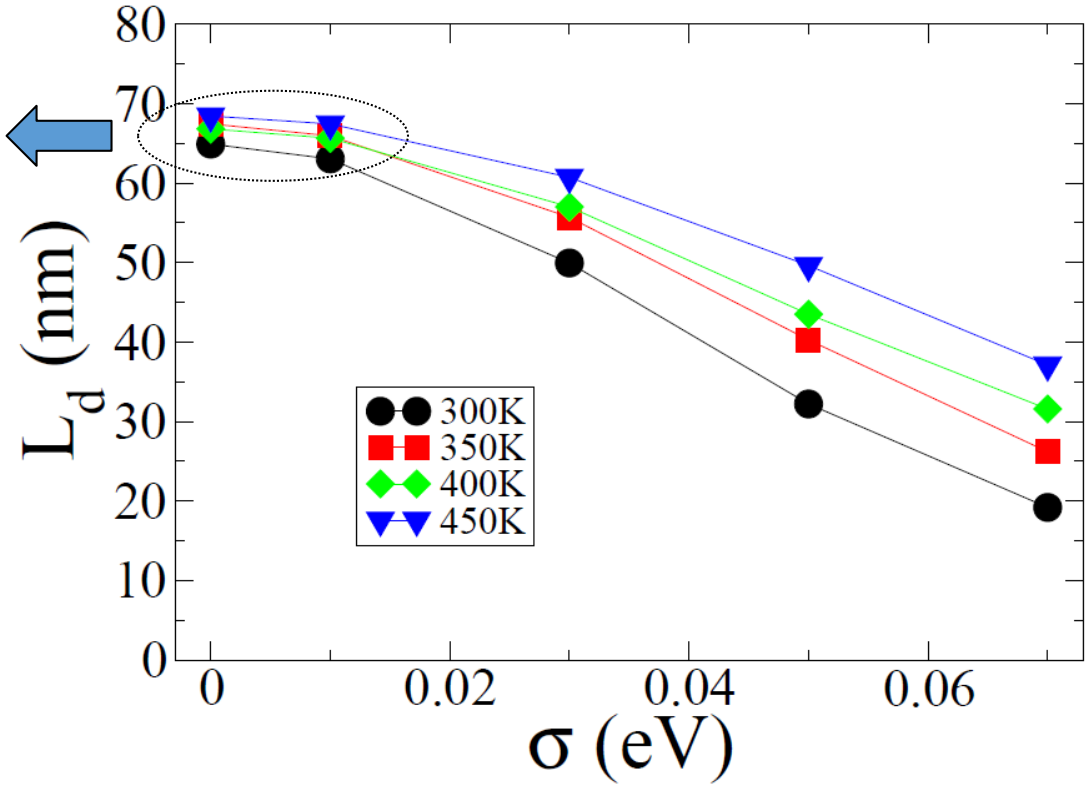

However, an inhomogeneous broadening of only 0.014 eV has been reported for similar step ladder type paraphenylene oligomers [Wiesenhofer et. al. *Adv. Funct. Mater.* 18, 310 (2006)].

Conclusions of Part II

- In this work we have studied the influence of morphology on exciton dynamics.
- We have looked at the temperature dependence of exciton diffusion and found that the diffusion length does not depend on T.
- Positional/orientational disorder doesn't seem to have a strong effect on the diffusion length, showing that temperature is not a limitation to exciton diffusion dynamics.
- Liquid crystalline oligomeric materials could be promising candidates to engineer optoelectronic devices that require stable and controlled electronic properties over a wide range of temperatures and supramolecular arrangements.

Acknowledgements

Part I

Dr. Hong Li, Georgia Tech, USA

Prof. Jean-Luc Brédas, Georgia Tech, USA

Dr. Jens Meyer, Princeton, USA

Prof. Antoine Kahn, Princeton, USA

Part II

- Prof. Alison Walker, Bath, UK
- Dr. Luca Muccioli, Bologna, IT
- Dr. Stavros Athanasopoulos, Mons, BE
- Prof. David Beljonne, Mons, BE

Department of
Natural Sciences